The kinetics and mechanism of the phosphorus-catalysed dimerisation of acrylonitrile

C. Dennis Hall,*[a] Nicholas Lowther,[a] Bruce R. Tweedy,[a] Adam C. Hall[a] and Gordon Shaw[b]

[a] *Dept. of Chemistry, King's College, Strand, London, UK WC2R 2LS*
[b] *ICI, Chemicals and Polymers, PO Box 90, Wilton, Middlesbrough, Cleveland, UK TS6 8JE*

Isopropyl diarylphosphinites (Ar_2POPr^i) catalyse the dimerisation of acrylonitrile (AN) to a mixture of *cis*- and *trans*-1,4-dicyanobut-1-ene (*cis*,*trans*-DCB-1), *trans*-1,4-dicyanobut-2-ene (DCB-2) and 2,4-dicyanobut-1-ene (MGN). The kinetics and mechanism of the reaction, which is a potential source of hexamethylenediamine, are reported in detail and the factors which govern rate and selectivity to DCB-1 and DCB-2 rather than MGN are elaborated.

Introduction

The dimerisation of acrylonitrile (AN, **1**) gives either 2,4-dicyanobut-1-ene (MGN, **2**) or *cis*- and *trans*-1,4-dicyanobut-1-ene (DCB, **3**) as the principle product and hydrogenation of the latter, *via* a two stage process, leads to hexamethylenediamine, a vital intermediate en route to Nylon 66. Thus the selective, catalysed dimerisation of AN to DCB is potentially a very important process which has been achieved using a variety of tricoordinate organophosphorus compounds (**4**) as homogeneous catalysts.[1–4]

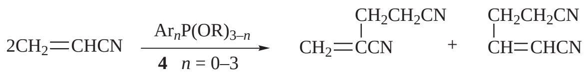

$$\underset{\mathbf{1}}{2CH_2{=}CHCN} \xrightarrow[\mathbf{4}\quad n = 0\text{–}3]{Ar_nP(OR)_{3-n}} \underset{\mathbf{2}}{CH_2{=}\overset{\overset{\displaystyle CH_2CH_2CN}{|}}{C}CN} + \underset{\mathbf{3}}{\overset{\overset{\displaystyle CH_2CH_2CN}{|}}{C}H{=}CHCN}$$

The successful exploitation of the dimerisation reaction as a commercial process, however, depends upon a knowledge of the optimum combination of rate, selectivity and turnover for the catalyst system. This paper describes structural and kinetic studies which elucidate the mechanism of the reaction and hence define the operational window for maximum catalytic efficiency.

Experimental

Instrumentation

^{31}P, ^{13}C, ^{19}F, ^{2}H and high resolution ^{1}H NMR spectra were obtained using a number of Fourier-transform multinuclear spectrometers (Bruker WM 250, Bruker AMX 400 and JEOL JNM-FX 200) operating at 250, 400 and 200 MHz (^{1}H) respectively.

Analytical GC was effected using several chromatographs all equipped with flame ionisation detectors. At ICI (Chemical and Polymers), three instruments were used: a Pye-Unicam series 104 GC, equipped with FID, a PD10 GC computer and teletype printer or two internally constructed GCs with integrators linked to a PDP-11 GC, minicomputer and a 32k Commodore PET computer and printer. One instrument was fitted with carrier gas backflush system to remove high boiling fractions. At King's College a Perkin-Elmer model 8310 GC equipped with a data handling station was used in conjunction with a Perkin-Elmer 8300 autosampler and printer. An in-line carrier gas purification system comprising a 50 cm by 3 cm copper column packed with reduced BASF R3-11 oxygen-removing catalyst and an Alltech 4004 indicating oxytrap was used. Preparative GC was effected using a Pye-Unicam series 105 Mk. 2 automatic preparative chromatograph. Mass spectra were obtained by the ULIRS service at the School of Pharmacy, London. Some distillations were carried out using a Buchi GKR-50 Kugelrohr apparatus in which case the boiling points reflect the oven temperature rather than the true values.

Solvents

All solvents were dried by standard methods,[5] distilled and stored under nitrogen over molecular sieves prior to use.

Tricoordinated phosphorus compounds

All the tricoordinated compounds used throughout this study were obtained or prepared and characterised by methods described in earlier publications.[6–9]

Preparation of 2-cyanoethyldiphenylphosphine

Two methods were used successfully.

(a) Phenylsilane reduction of 2-cyanoethyldiphenylphosphine oxide. Phenylsilane (0.38 g, 3.5 mmol) was added to 2-cyanoethyldiphenylphosphine oxide (2.03 g, 8.0 mmol). The reaction mixture was maintained under reflux at 100 °C for 2 h. After cooling, the residue was distilled (Kugelrohr) to give 1.10 g (57%) of a colourless liquid (bp 170–175 °C, 0.3 mmHg) which crystallised on standing to yield a white solid of mp 63–64 °C (lit.,[10] 64–64.5 °C). $\delta_P(C_6D_6)$ −16.1, $\delta_H(CDCl_3)$ 2.38 (m, 4H) and 7.40 (m, 10H).

(b) The condensation of diphenylphosphine with acrylonitrile. Diphenylphosphine (9.9 g, 53 mmol) and acrylonitrile (3.6 g, 71 mmol) were introduced to a tube cooled to −78 °C under an atmosphere of nitrogen. The tube was sealed and heated to 130 °C for 7.5 h. The excess volatiles were removed from the reaction mixture under reduced pressure to leave a dark oil which semi-crystallised on standing. This was distilled (Kugelrohr) to give a colourless liquid (bp 170–180 °C, 0.19 mmHg) which crystallised on standing to yield 8.90 g (70%) of a white solid of mp 63–64 °C (lit.,[11] 64–64.5 °C). $\delta_P(CDCl_3)$ −16.2, $\delta_H(CDCl_3)$ 2.39 (m, 4H) and 7.40 (m, 10H).

Preparation of 2-cyanoethyldiphenylphosphine oxide

Acrylonitrile (6.64 g, 0.125 mol) was added, dropwise with stirring under nitrogen, to a cooled (0 °C) solution of diphenylphosphine oxide (21.80 g, 0.108 mol) and potassium hydroxide (10 M aqueous solution, 8 ml) in acetonitrile (30 ml). Stirring was continued for a further 2.5 h, during which time the reaction vessel was allowed to warm to ambient temperature and the mixture was then allowed to stand at ambient temperature for a further 48 h. The reaction mixture was washed with potassium hydroxide solution (10 M, 3 × 10 ml) water (3 × 20 ml) and the organic layer was separated and dried ($MgSO_4$). The volatiles were removed, under reduced pressure, to leave a brown oil which was triturated with diethyl ether (250 ml). The resultant white, crystalline solid was collected and recrystallised from benzene–hexane to yield 25.2 g (90%) of the product as fine white crystals, mp 101–102 °C (lit.,[12] 102–103 °C). $\delta_P(C_6D_6)$ +25.8, $\delta_H(CDCl_3)$ 2.74 (m, 4H) and 7.70 (m, 10H).

Acrylonitrile

Commercial acrylonitrile (Aldrich) was dried (×2) over crushed calcium hydride, degassed and distilled onto freshly activated 3 Å molecular sieves under an atmosphere of nitrogen.

Kinetic procedures

GC and high resolution ^{1}H and ^{2}H NMR were used as the analytical tools in the evaluation of the kinetic parameters k_1, K_2 and k_8/k_5.

The monitoring of [AN], [MGN], [DCB] and [trimer] at King's College London

Toluene (20 ml), AN (6 ml, 9×10^{-2} g mol) and isopropanol (IPA, 2 ml, 2.66×10^{-2} g mol) were introduced to a glass vessel which was sealed (Subaseal) under an atmosphere of nitrogen. The flask was thermostatted at 60 °C in an oil bath for 15 min. An aliquot of phosphinite catalyst (2 mmol, *ca.* 500 µl) was introduced to the thermostatted reaction mixture using a gas-tight microsyringe with shaking to effect complete solution. Aliquots of the reaction mixture (500 µl) were removed periodically and were added to solutions of 0.01 M HCl (6 µl) in acetone (300 µl) containing dimethyl phthalate (10 µl) in GC microvials. The vials were sealed with crimped caps and were shaken throughly. This process deactivated the catalyst by solvolysis and introduced a 'low boiler' internal standard (acetone) and a 'high boiler' internal standard (dimethyl phthalate) to each sample. These samples were analysed on a Perkin-Elmer 8310 GC with an integral data handling station linked to a Perkin-Elmer 8300 autosampler. A 1 m × $\frac{1}{4}''$ od glass column packed with Ultrabond 20 M 100/120 mesh was used. The carrier gas flow rate was 9 ml min^{-1}. The temperature program was as follows: 40 °C isothermal (8 min) followed by a ramp (10 °C min^{-1}) to 130 °C with a further isothermal period (15 min) followed by a second ramp (5 °C min^{-1}) to 240 °C with a final isothermal period of 55 min. The injector block temperature was 270 °C and the detector temperature was 300 °C. Peaks were eluted in the order: acetone, IPA, AN, toluene, MGN, *cis*-DCB-1, dimethyl phthalate, *trans*-DCB-1, trimer, solvolysed catalyst and a typical chromatogram is displayed in Fig. 1. The amount of DCB-2 formed in the reaction was small (generally <2%) and with this GC method was only detectable as a shoulder (at *ca.* 19.5 min) on the peak due to *trans*-DCB-1. With the aid of the two internal standards the raw GC data were converted into [AN], [MGN], [DCB] and [trimer] *vs.* time data.

The analysis of the total product distribution at ICI Chemicals and Polymers

Toluene (10 ml), AN (3 ml) and IPA (1 ml) were loaded into a glass vessel and were sealed under nitrogen. The flask was thermostatted at 60 °C for 15 min. An aliquot of phosphinite catalyst (1 mmol, *ca.* 250 µl) was introduced to the thermostatted reaction mixture using a gas-tight microsyringe with shaking to effect complete solution. At the required level of AN conversion the reaction was 'killed' by the addition of water (1 ml) and methanol (1 ml) which deactivated the catalyst by solvolysis. The resulting mixture was passed through a preweighed sintered filter in order to collect any crystalline hexamer. The sinter was dried to constant weight. The low boiling materials were removed from the filtrate under reduced pressure (*ca.* 20 mm) at temperatures of 30–50 °C. There remained an oily residue containing dimeric species, low molecular weight oligomers and 'dead' catalyst; the weight of this residue was recorded. A weighed aliquot (*ca.* 0.1 g) of the 'oils' was added to a weighed quantity of dimethyl phthalate (*ca.* 0.1 g) in acetone (*ca.* 10 ml). The resulting sample was analysed by GC using a 2.5 cm × $\frac{1}{8}''$ od stainless steel (ss) column of 7.5% LAC 2R-446 on Chromosorb WH-P treated with 0.5% H_3PO_4. The primary carrier gas pressure was 30 psi. The injector block temperature was 180 °C and the oven temperature was 190 °C. Peaks were eluted in the order: solvent, MGN, *cis*-DCB-1, dimethyl phthalate, and *trans*-DCB-1 (plus DCB-2). Each analysis was performed in triplicate to check for consistency. With the aid of the internal standard (dimethyl phthalate) the total product distribution was quantified enabling percentage selectivities of each product to be calculated. Oligomer quantities were assessed on the basis of 'non-GC accountables', *i.e.* by a weight difference method.

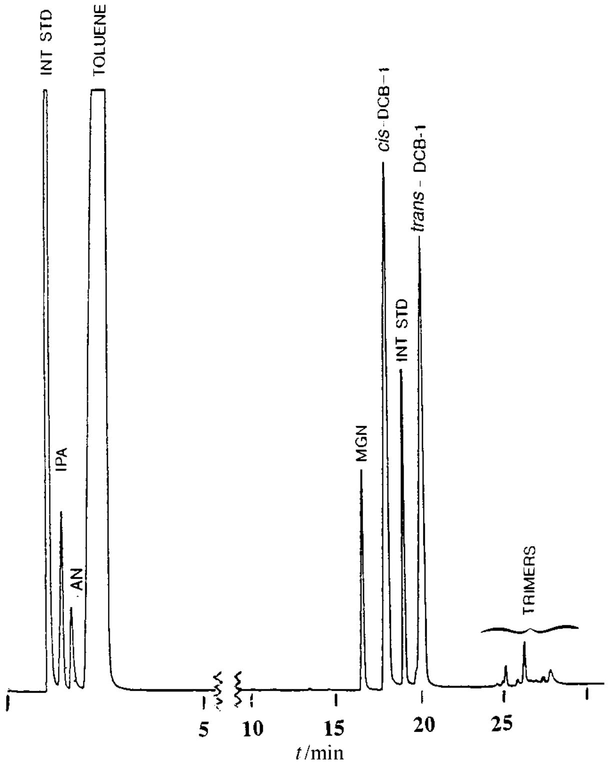

Fig. 1 A typical gas chromatogram of the AN dimerisation mixture

The monitoring of [AN] at ICI Chemicals and Polymers

Toluene (10 ml), AN (3 ml) and IPA (1 ml) together with *n*-heptane (1 ml) were loaded into a glass vessel which was sealed under nitrogen and the flask was thermostatted at 60 °C for 15 min. An aliquot of phosphinite catalyst (1 mmol, *ca.* 260 µl) was introduced to the reaction mixture using a gas-tight microsyringe with shaking to effect complete solution. Small aliquots (*ca.* 1–2 µl) were extracted periodically from the reaction mixture and were analysed by GC using a 2.5 m × $\frac{1}{8}''$ od ss column of silicon OV-225 with a pre-column of 7.5% LAC 2R-446 on Chromosorb WH-P treated with 0.5% H_3PO_4. A carrier gas backflush mechanism was fitted to the system to remove higher boilers. The primary carrier gas pressure was 7 psi, the injector block temperature was 70 °C and the oven temperature was 80 °C. Peaks were eluted in the order: *n*-heptane, IPA, AN, toluene. The *n*-heptane was employed as an internal standard and the raw GC data were converted into [AN] *vs.* time data.

The monitoring of [MGN] and [DCB] at ICI Chemicals and Polymers

Toluene (10 ml), AN (3 ml) and IPA (1 ml) together with adiponitrile (0.2 ml) were loaded into a glass vessel which was sealed under nitrogen. The flask was thermostatted at 60 °C for 15 min and an aliquot of phosphinite catalyst (1 mmol, *ca.* 250 µl) was introduced using a gas-tight microsyringe with shaking to ensure complete solution. Small aliquots (*ca.* 1–2 µl) were periodically extracted from the reaction mixture and were analysed on a Pye-Unicam series 104 GC using a 1.5 m × $\frac{1}{4}''$ od glass column containing 7.5% LAC 2R-446 Chromosorb WH-P treated with 0.5% H_3PO_4. The primary carrier gas pressure was 16 psi, the injector block temperature was 170 °C and the oven temperature was 185 °C. Peaks were eluted in the order: solvent, MGN, *cis*-DCB-1, adiponitrile, *trans*-DCB-1 (+ DCB-2). The adiponitrile was employed as an internal standard for quantitation and the raw GC data were converted into [MGN] and [DCB] *vs.* time data.

The incorporation of deuterium into unreacted AN

Toluene (10 ml), AN (3 ml) and IPA-OD (1 ml or in preliminary experiments, 4 ml) were loaded into a glass vessel and sealed under nitrogen. The flask was thermostatted at 60 °C for 15 mn and an aliquot of phosphinite catalyst (1 mmol, *ca.* 250 µl) was introduced using a gas-tight microsyringe with shaking to ensure complete solution. A number of reactions were set up under these conditions and at different percentage conversions of AN the reactions were 'killed' by the addition of water (1 ml) and methanol (1 ml). Each reaction mixture was filtered to remove the crystalline hexamer by-product. The low boiling materials were removed from the filtrates under reduced pressure (*ca.* 20 mm) and were collected in a cold (−78 °C) trap. Both the low boiling and the high boiling fractions from each reaction were separated on a Pye-Unicam series 105 Mark 2 automatic preparative chromatograph prepared with a 1.5 m × $\frac{1}{4}''$ od glass column containing 7.5% LAC 2R-446 on Chromosorb WH-P treated with 0.5% H_3PO_4. For the low boiling fractions the oven temperature was 70 °C and the primary carrier gas pressure was 8 psi. For the high boiling fractions the oven temperature was 190 °C and the primary carrier gas pressure was 20 psi. Using these conditions the partially deuteriated unreacted AN was collected from each reaction and assessed by high resolution ^1H and ^2H NMR spectroscopy.

The incorporation of hydrogen into unreacted deuterioacrylonitrile[13]

Deuteriotoluene (0.5 ml), deuterioacrylonitrile (0.15 ml) and IPA (0.05 ml) were loaded into a 5 mm NMR tube and the mixture was thermostatted at 60 °C for 15 min. An aliquot of phosphinite catalyst (0.05 mmol, *ca.* 13 µl) was introduced using a gas-tight microsyringe with shaking to ensure complete solution. The reaction was monitored by high field (250 MHz) ^1H NMR in the thermostatted (60 °C) probe of a Bruker WM250 instrument. The levels of protonation in the unreacted AN were assessed using the methyl resonance signals in the IPA as an internal standard.

Results and discussion

The mechanistic pathway proposed for the formation of dimers **2** and **3** is shown in Scheme 1. In addition the reaction affords a number of by-products including 1,4-dicyanobut-2-ene, a variety of trimeric species and a crystalline hexamer $(CNCH_2CH_2)_2C(CN)CH{=}CHC(CN)(CH_2CH_2CN)_2$ in quantities dependent upon the reaction conditions and the catalyst used. Although no betaine (B) or ylide (Y) intermediates were observed by NMR, the intermediacy of the ylide species was established by trapping the latter with benzaldehyde.[1b] The kinetics of the reaction were studied by monitoring the rate of disappearance of AN and the rate of appearance of DCB or MGN by gas-liquid chromatography (GLC) on a capillary column which was also capable of analysing the reaction mixtures quantitatively for trimers. Any crystalline hexamer formed was filtered off and estimated gravimetrically. Independent experiments showed that the hexamer was derived from either DCB-1 or DCB-2 and that the trimers (and oligomers) were derived in a consecutive fashion from dimers and AN rather than in a parallel manner from B^2 or B^3 plus AN (see Scheme 1). Thus a plot of [trimer] *vs.* % conversion of AN gave an S-shaped curve (Fig. 2) consistent with consecutive formation of the trimer from dimers and AN.

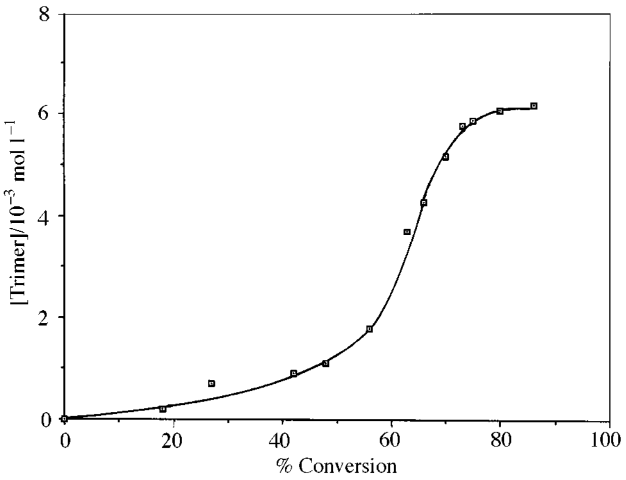

Fig. 2 A plot of [trimer] *vs.* % conversion; 10 : 3 : 1 (v/v) ratio of toluene : AN : IPA, at 333 K; [catalyst] = 0.037 M

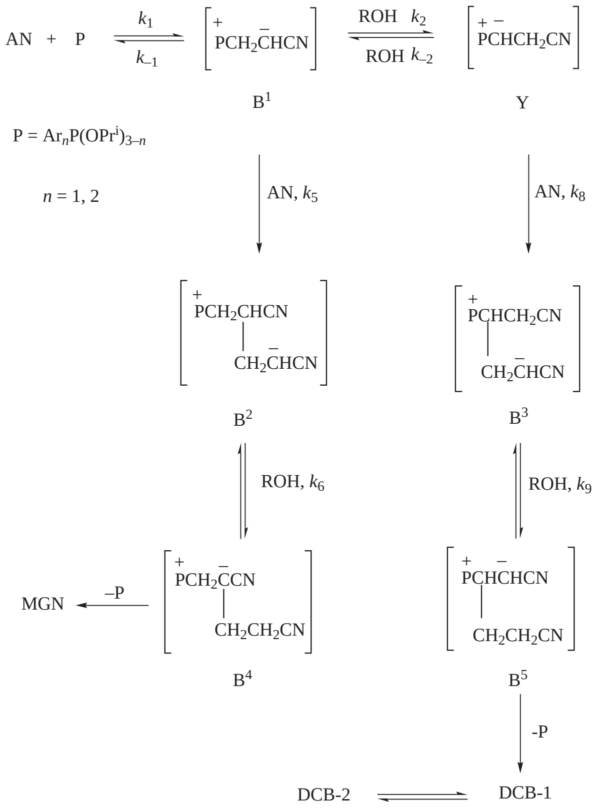

Scheme 1

A similar plot was observed for the formation of hexamer again indicating a consecutive process. Deliberate loading of mixtures of AN and the individual dimers gave relative rate data for the formation of hexamer and trimer under dimerisation conditions (Table 1). Thus one may envisage formation of hexamer, trimer and higher oligomers from DCB-1, DCB-2 and MGN *via* the routes shown in Scheme 2, where the base (B) is probably the initial betaine B^1 or the ylide, Y.

$$\left.\begin{array}{l}\text{DCB-1} + \text{Base (B)} \rightleftharpoons NCCH_2\bar{C}HCH{=}CHCN \\ \text{DCB-2} + \text{B} \rightleftharpoons NCCH_2CH{=}CH\bar{C}HCN\end{array}\right\}\begin{array}{l}\xrightarrow{4AN} \text{Hexamer} \\ \quad\text{or} \\ \xrightarrow{AN} \text{Trimer}\end{array}$$

$$\text{MGN} + \text{B} \rightleftharpoons CH_2{=}C(CN)CH_2\bar{C}HCN \xrightarrow{AN} \text{Trimer } \textit{etc.}$$

Scheme 2

Table 1 Relative rates of formation of the hexamer and trimers from DCB-2, DCB-1 and MGN under standard dimerisation conditions[a]

Dimer	Relative rates under dimerisation conditions Hexamer formation	 Trimer formation
trans-DCB-2	12	7
cis-DCB-1	5	4.5
trans-DCB-1	1	1
MGN	0	4

[a] *T* 60 °C. In 10 : 3 : 1 (v/v) toluene–AN–IPA; catalyst, Ph_2POPr^i.

Table 2 k_{obs} *vs.* $[P^{III}]$ obtained using [AN], *f*[MGN] and *f*[DCB] data[a]

[Catalyst]	K_2k_8/k_5	$k_{obs}/10^{-5}$ s^{-1} obtained using [AN]	 *f*[MGN]	 *f*[DCB]
0.0426	18.9	1.06	0.90	0.90
0.0515	20.6	—	1.28	1.28
0.0618	18.9	1.52	1.67	1.67
0.0741	18.8	1.71	1.74	1.75
0.0754	20.8	2.18	1.91	1.92
0.124	19.9	3.23	3.19	3.19
0.146	18.9	3.72	3.57	3.57

[a] *T* 60 °C. In 10 : 3 : 1 (v/v) toluene–AN–IPA; catalyst, Ph_2POPr^i.

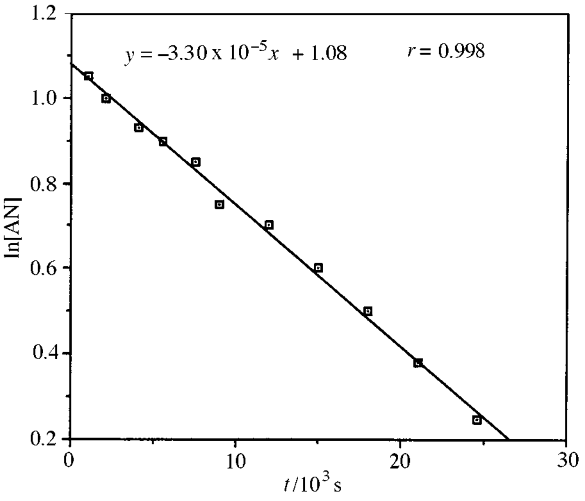

Fig. 3 A typical plot of ln[AN] *vs.* *t* (s)

Table 3 Average k_1, K_2k_8/k_5, k_8/k_5 and K_2 values for a series of phosphinite catalysts $(XC_6H_4)(X'C_6H_4)POPr^i$[a]

Catalyst	K_2k_8/k_5	K_2	k_8/k_5	$k_1/10^{-4}$ l mol^{-1} s^{-1}	$\Sigma\sigma$
X = X′ = *p*-F	23.1	2.29	10.1	0.64	0.120
X = X′ = H	19.0	2.02	9.4	2.57	0
X = X′ = *m*-Me	15.3	1.55	9.9	4.85	−0.138
X = H, X′ = *p*-Me	16.7	1.65	10.1	5.34	−0.170
X = H, X′ = *p*-MeO	14.2	1.35	10.5	8.16	−0.268
X = H, X′ = *p*-Pr^iO	13.8	1.47	9.4	7.20	−0.290
X = H, X′ = *p*-Et_2N	7.58	1.01	7.5	77.1	−0.700
X = X′ = *o*-MeO	1.32	1.37	0.96	3.60	—

[a] *T* 60 °C. In 10 : 3 : 1 (v/v) toluene–AN–IPA.

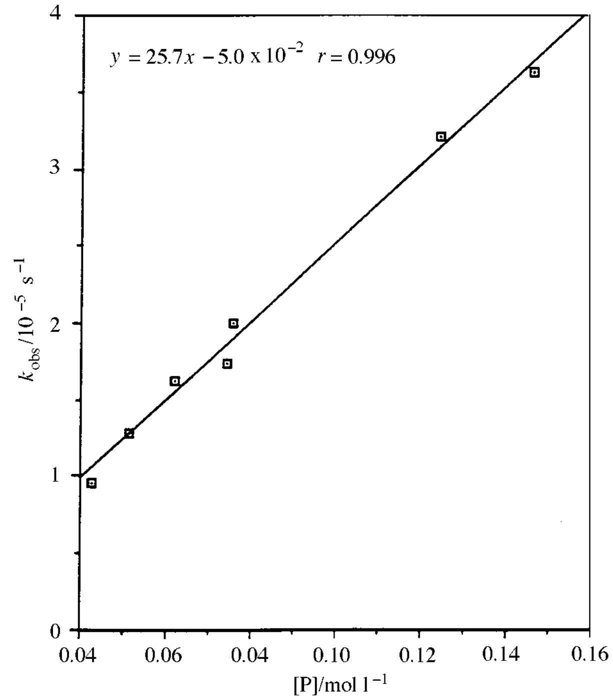

Fig. 4 Plot of k_{obs} *vs.* [phosphinite]; 10 : 3 : 1 (v/v) ratio of toluene : AN : IPA, at 333 K; catalyst Ph_2POPr^i

Having established the rates of formation of by-products under any set of dimerisation conditions it was possible to correct concentrations of AN, DCB or MGN observed in the reaction mixtures at any time, *t*, for the formation of hexamer or trimers. Assuming k_5[AN] and k_8K_2[AN] of Scheme 1 are both $\gg k_{-1}$ (justified by deuterium exchange studies, *vide infra*) the SSO may be applied to B^1 and Y from which eqn. (1) may be

$$-d(AN)/dt = 2k_1 [P][AN] \qquad (1)$$

derived. Thus a plot of ln [AN] *vs.* *t* should give a slope = $2k_1$[P] where [P] is the constant phosphorus catalyst concentration. Furthermore, for the formation of MGN and DCB the appropriate integrated rate expressions (see Appendix) are given by eqns. (2) and (3).

$$\ln \{[AN]_0 - 2[MGN](1 + k_8K_2/k_5)\} = 2k_1[P]t \qquad (2)$$

$$\ln \{[AN]_0 - 2[DCB](1 + k_5/k_8K_2)\} = 2k_1[P]t \qquad (3)$$

Thus plots of ln *f*[MGN] *vs.* *t* and ln *f*[DCB] *vs.* *t* where *f*[MGN] and *f*[DCB] are given by eqns. (2) and (3), respectively, should also give slopes = $2k_1$[P]. In fact it was found that, provided [AN], [MGN] and [MCB] were all corrected for hexamer and trimer formation, the logarithmic plots *vs.* time all gave excellent linear correlations (*e.g.* Fig. 3 for AN data) and the resultant values for k_{obs} using a range of concentrations of Ph_2POPr^i as catalyst are shown in Table 2. A plot of the average k_{obs} values from reactant product monitors *vs.* catalyst concentration [P] gave a linear correlation (Fig. 4) with slope = $2k_1$. Thus the kinetics of dimerisation were shown to be first order in AN and catalyst.

The value of K_2k_8/k_5 was taken as the ratio of DCB–MGN found in the product and is seen (Table 2) to be independent of the *concentration* of catalyst used but dependent upon the *nature* of the catalyst (Table 3). Table 3 shows quite clearly that as the reactivity of the catalyst increases, from X = X′ = *p*-F to X = H, X′ = *p*-NEt_2, the selectivity to DCB decreases by a factor of *ca.* 3. A plot of log K_2k_8/k_5 *vs.* σ gave a good linear correlation ($r = 0.992$) with $\rho = +0.58$ showing that the selectivity to DCB is increased by electron withdrawal in the aryl groups of the phosphinite catalyst. Since the experimental ρ value is a composite of K_2 ($+\rho$), k_8 ($-\rho$) and k_5 (probably a small $-\rho$ value) it is apparent that the selectivity is dominated by the equilibrium between the betaine B^1, and the ylide Y, of Scheme 1.

An attempt was made to evaluate K_2 independently from the ratio of H^A (or H^B) to H^X (Scheme 3) incorporated into un-

Table 4 The incorporation of hydrogen into unreacted $[^2H_3]$AN *vs.* % conversion[a]

% AN conversion	% H incorporated			
	H^A	H^B	H^X	$\frac{1}{2}(H^A + H^B)/H^X$
2.2	0.21	0.20	0.13	1.62
3.8	0.43	0.39	0.27	1.56
8.1	0.51	0.67	0.30	1.97
11.9	1.13	1.16	0.45	2.54
14.6	1.33	1.38	0.60	2.25
19.4	1.67	1.65	0.50	3.32
23.7	2.47	2.42	1.27	1.93
28.6	2.27	2.27	1.37	1.66
32.4	3.17	3.03	1.78	1.75
38.9	3.26	3.41	2.17	1.62

[a] *T* 60 °C. In 10:3:1 (v/v) toluene–$[^2H_3]$AN–IPA; catalyst Ph_2POPr^i (0.073 M).

Table 5 Incorporation of deuterium into unreacted AN *vs.* % conversion of AN[a]

% Conversion	% D incorporated			
	H^A	H^B	H^X	$\frac{1}{2}(H^A + H^B)/H^X$
5.0	0.63	0.79	0.23	3.09
11.6	0.74	0.92	0.43	1.93
16.8	1.45	1.53	0.68	2.19
17.3	1.60	1.50	0.63	2.58
28.2	1.71	1.60	0.61	1.64
40.2	2.36	2.66	0.89	2.82

[a] *T* 60 °C. In 10:3:1 (v/v) toluene–AN–IPA-OD; catalyst Ph_2POPr^i (0.073 M).

Table 6 Deuterium uptake in *cis*-DCB-1 by ^{2}H NMR[a]

% AN conversion	% D incorporated				
	H^A	H^X	H^C	H^D	H^A/H^X
5.0	45.9	29.2	3.5	20.2	1.57
11.6	58.3	37.1	3.9	26.4	1.57
16.8	51.4	32.2	4.0	24.5	1.60
17.3	47.3	32.6	3.2	20.0	1.45
18.1	42.4	27.0	3.1	17.8	1.57
28.2	35.3	23.7	2.9	15.1	1.49
40.2	27.0	17.0	4.0	12.5	1.59
44.2	25.2	14.7	2.6	11.0	1.71

[a] *T* 60 °C. In 10:3:1 (v/v) toluene–AN–IPA-OD; catalyst Ph_2POPr^i (0.073 M).

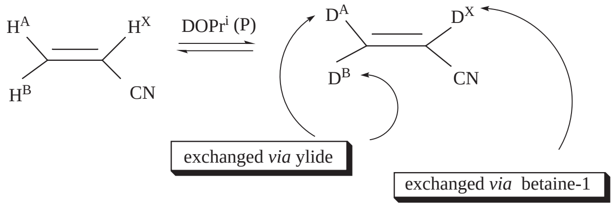

Scheme 3

reacted $[^2H_3]$AN (Table 4) or the incorporation of D into unreacted AN (Table 5) over a range of conversions from 2 to 40%. K_2 was found to be about 2 for Ph_2POPr^i but this varied with the nature of the catalyst (Table 3). The evaluation of K_2 is rationalised as follows. It is obvious that there are potentially eight separate species (**5**–**12**) in the partially deuterated AN. All except **12** could be observed separately in the resolution enhanced 400 MHz ^{1}H NMR spectrum of unreacted AN. The level of deuterium incorporation into **6**–**11** could therefore be assessed by integration and the level of deuterium incorporated at all three sites (represented by **12**) was estimated as one third of the average of **9**–**11**. A plot of % of theoretical D (or H) incorporated *vs.* % conversion of AN was linear with a slope of *ca.* 2.5 indicating that all the available D (or H) would be exchanged at *ca.* 40% AN conversion. Thereafter the species in solution could be expected to equilibrate slowly with H/D available in solution. The analysis generated the data in Table 5 and it was checked by ^{2}H NMR (at 30.6 MHz) of the partially deuterated AN which gave three distinct signals for D^A, D^B and D^X integrating for the same ratio of D^A/D^X or D^B/D^X as observed from the ^{1}H data. The experiment was repeated in reverse by observing the incorporation of ^{1}H into $[^2H_3]$AN which gave the data recorded in Table 4. Although there is some scatter, it is clear that the two sets of data agree in terms of the ratio of exchanged H^A/H^X or H^B/H^X with an average value of *ca.* 2 using Ph_2POPr^i as catalyst. Incorporation of D (or H) into sites A and B must occur through an ylide structure and incorporation of D (or H) into site X together with the reverse reaction to regenerate AN, must occur through a betaine structure. If the betaine–ylide equilibrium was fast and the H/D exchange at all three sites was also fast relative to the reverse reaction or the onward reaction to MGN or DCB then the exchange observed within sites A, B and X of unreacted AN would be the same and should merely reflect the amount of D (or H) available from the alcohol solvent. In fact, using Ph_2POPr^i as catalyst, the amount of H incorporated in sites A and B of $[^2H_3]$AN is approximately twice that in site X. This observation might be ascribed to a deuterium isotope effect on the reverse (elimination) step but such an argument is negated by the fact that incorporation of D into unreacted AN also gives more D in sites A and B than in site X whereas a deuterium isotope effect on the elimination would have predicted the opposite. Incidentally, this suggests that the elimination to regenerate AN occurs *via* an E1cB mechanism with little or no isotope effect (*vide infra*). An examination of the incorporation of H (or D) in isolated *cis*- or *trans*-DCB-1 (**13a** or **13b**) from $[^2H_3]$AN (or AN) gave a similar result. Using ^{2}H NMR† the average ratio of D^A/D^X up to 44% conversion was 1.5 in *cis*-DCB-1 (Table 6) and 1.7 in *trans*-DCB-1 (Table 7). The average ratio (1.60) is slightly lower than that observed for unreacted AN (*ca.* 2) but this may be explained by a small deuterium isotope effect on the final intra- or inter-molecular elimination step to form DCB-1 (Scheme 4). The k_H/k_D value for this pro-

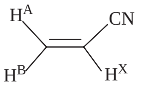

5

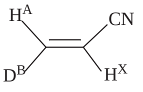

6

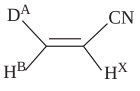

7

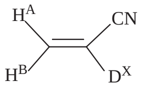

8

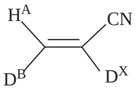

9

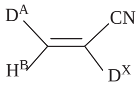

10

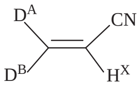

11

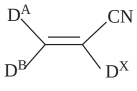

12

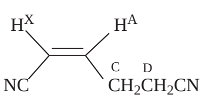

13a

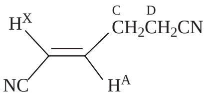

13b

---

† The results from the incorporation of D into DCB derived from $[^1H_3]$AN were particularly useful since with *cis*-DCB-1, four distinct ^{2}H signals were observed for D^A, D^X, D^C and D^D although with *trans*-DCB-1 only three distinct signals were observed since D^C and D^D overlapped.

Table 7 Deuterium intake in *trans*-DCB-1 by ^2H NMR[a]

% AN conversion	% D incorporated			
	H^A	H^X	$(H^C + H^D)^b$	H^A/H^X
5.0	39.1	23.8	13.0	1.64
11.6	42.4	26.4	15.4	1.61
17.3	44.5	26.5	11.4	1.68
18.1	26.8	15.4	8.0	1.74
28.2	30.4	18.0	8.9	1.69
40.2	22.6	12.4	7.1	1.82
44.2	22.8	11.4	6.3	2.00

[a] *T* 60 °C. In 10:3:1 (v/v) toluene–AN–IPA-OD; catalyst Ph_2POPr^i (0.073 M). [b] Not observable as separate signals.

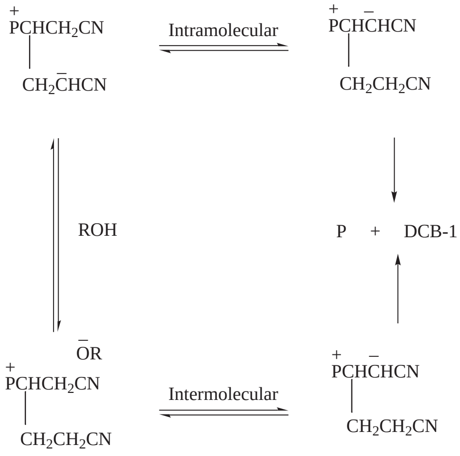

Scheme 4

cess may be approximated by comparing the ratio of H^A, H^B/H^X for the reverse reaction with that of the elimination to DCB, giving a k_H/k_D value for the latter process of *ca.* 1.3 (2/1.6) consistent with an E1cB mechanism.

Thus we are faced with a situation where more H (or D) is incorporated in sites A and B (*via* ylide) than in site X (*via* betaine) and this suggests kinetic control of a process in which the rate of exchange at all three sites is determined by the *relative concentrations* of ylide and betaine. In other words there is competition for the unstable betaine and ylide intermediates between a reversal to starting materials (*via* the betaine), H/D exchange with the alcohol and reaction with more AN to form dimers. This is a reasonable hypothesis since the alcohol concentration remains constant throughout and $k_{exchange}$ values for ylide or betaine are likely to be very similar if not identical. As pointed out by a referee however, this analysis to extract K_2 is clearly only valid if the equilibration of betaine and ylide does not involve proton (or deuteron) transfer *via* alcohol as depicted in Scheme 5a. An alternative which does not involve proton transfer (Scheme 5b) is feasible but if Scheme 5a (the expected pathway) is correct, the amounts of H (or D) at sites A/B *vs.* X would only be an indication of the relative concentrations of ylide and betaine an hence an indication of the *trend* in K_2 as the substituent, X, was varied. The values of K_2 and k_1 vary with the catalyst (Table 3) and Hammett plots gave *ρ*-values (against *σ*) of −2.3 for k_1 (Fig. 5, $r = 0.99$) and +0.4 (±0.2) for K_2 ($r = 0.974$). The k_8/k_5 ratio however, remained fairly constant throughout except for the *o*-MeO substituent (*vide infra*).

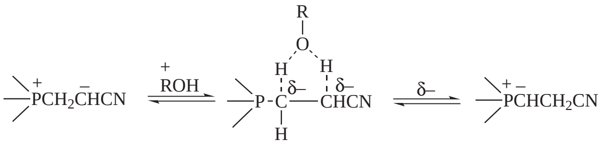

Scheme 5a

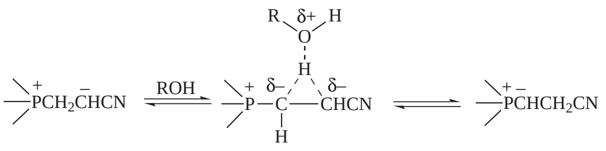

Scheme 5b

Table 8 Activation parameters for the dimerisation of AN[a] at [P] = 0.073 M

Catalyst	k_1 (60 °C)/10^{-4} l mol^{-1} s^{-1}	E_A/kcal mol^{-1}	$\Delta S^\ddagger$(298 K)/cal mol^{-1} K^{-1}
$(p\text{-}Me_2NC_6H_4)_2POPr^i$	2300	10.3	−33
$(p\text{-}MeOC_6H_4)_2POPr^i$	27.1	6.8	−52
$(p\text{-}MeC_6H_4)_2POPr^i$	3.91	6.0	−56
Ph_2POPr^i	2.57	5.0	−64

[a] In 10:3:1 toluene–AN–IPA (v/v).

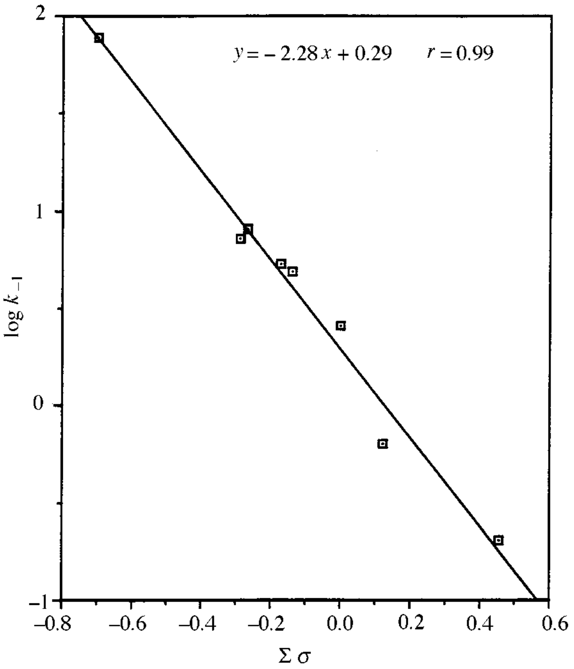

Fig. 5 Hammett plot of log k_1 *vs.* Σ*σ*

The data are entirely consistent with formation of the betaine as the rate-limiting step of the reaction with K_2 having a profound influence on the selectivity to DCB as the substituents in the aryl groups are changed. Thus increasing electron donation by X increases the rate of reaction (negative *ρ*) by stabilising the developing positive charge on phosphorus. Conversely, electron withdrawing groups stabilise Y relative to B^1 thus increasing K_2 (positive *ρ*) and hence increasing the selectivity to DCB as the rate of reaction decreases. The ratio k_8/k_5 remains essentially constant throughout the range of *meta*- and *para*-substituents but *ortho*-substituents in the phosphinite decrease the ratio of k_8/k_5 by an order of magnitude. This accounts for the low selectivity found with *ortho*-substituents which probably decrease the reactivity of the ylide by steric hindrance. The activation parameters (Table 8) indicate an associative rate-limiting step with the most reactive having the highest E_A value (10.3 kcal mol^{-1}) but the least negative $\Delta S^\ddagger$ value (−33 cal mol^{-1} K^{-1}). The isokinetic temperature for the dimerisation reaction is found to be *ca.* −100 °C. The effect of temperature on the ratio K_2k_8/k_5 was also investigated for a range of catalytic activity (Table 9). In general, lower temperatures are associated with higher selectivity so if we assume that the temperature coefficients for k_5 and k_8 are equal, the equilibrium between betaine and ylide (represented by K_2) is an exothermic process with $\Delta H°$

Table 9 Effect of temperature on the ratio K_2k_8/k_5 for a series of catalysts in 10 : 3 : 1 C_7H_8–AN–IPA (v/v)

	K_2k_8/k_5 at		
Catalyst	333 K	314 K	283 K
$(p\text{-}Et_2NC_6H_4)_2POPr^i$	2.9	3.4	4.1
$(p\text{-}Et_2NC_6H_4)PhPOPr^i$	9.7	11.8	14.2
$(p\text{-}MeC_6H_4)_2POPr^i$	14.0	17.3	21.3
Ph_2POPr^i	18.9	22.9	28.5

Table 10 k_{obs} values from [AN], f[MGN] and f[DCB] data in different solvent systems[a]

		$k_{obs}/10^{-5}$ s^{-1} obtained using		
Solvent system (v/v) toluene–AN–IPA–PN[b]	K_2k_8/k_5	[AN]	f[MGN]	f[DCB]
10 : 3 : 1 : 0	18.9	1.71	1.75	1.75
10 : 2.5 : 1 : 0.64	19.4	1.07	1.15	1.15
10 : 2 : 1 : 1.28	20.0	0.86	0.92	0.92
10 : 1.5 : 1 : 1.92	20.8	0.61	0.83	0.85
10 : 1 : 1 : 2.26	21.3	0.52	0.52	0.52

[a] T 60 °C; catalyst Ph_2POPr^i (0.073 M). [b] PN = propionitrile.

in the region of −2.0 kcal mol^{-1}. The composition of the reaction mixture may also be expected to change both reaction rate and selectivity.

This is illustrated in Table 10 where an attempt was made to keep the relative permittivity of the medium constant by addition of propionitrile. As the ratio of AN–IPA decreased, the selectivity of DCB increased but the rate of reaction (as denoted by k_1) decreased.

Thus any practical catalytic dimerisation system requires a compromise between reactivity and selectivity as controlled by the nature of the catalyst, the temperature window and the composition of the reaction mixture in terms of the relative amounts of AN and the proton transfer agent, IPA. It is reasonable to assume that the pentacoordinate structure of Scheme 6 might constitute an intermediate in the proton transfer process. In fact, this hypothesis is extremely unlikely since the dialkoxyphosphorane of Scheme 6 (Ar = Ph, R = Pr^i and $n = 2$) when prepared independently by the sulfenate ester route[6] failed to catalyse the dimerisation reaction under conditions identical to those used with Ph_2POPr^i. Thus the proton transfer is mediated by alcohol, preferably secondary and probably *via* an intermediate (or TS) depicted in Scheme 5a or 5b.

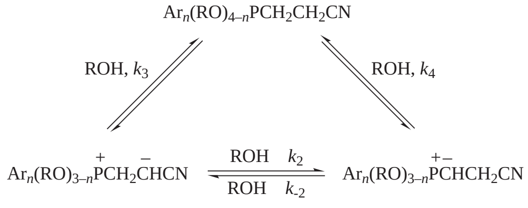

Scheme 6

It is clear from the data in Tables 4 and 5 that the first step of the reaction (with rate coefficient k_1) is reversible to a small extent. At *ca.* 40% conversion of AN to dimer, about 7.5% of the total available hydrogen (or deuterium) in sites H^A, H^B or H^X has been exchanged. The rate of exchange may then be used to estimate an observed rate coefficient (k_r) for the reverse reaction and values of the latter parameter as derived from H^A, H^B and H^X are shown for a range of catalysts in Table 11.

Table 11 k_r for a series of catalyst $XC_6H_4(X'C_6H_4)POPr^i$ loaded at 0.073 M in 10 : 3 : 1 (v/v) toluene–AN–IPA at 60 °C

	$k_r/10^{-5}$ s^{-1} obtained using			
Catalyst	H_A	H_B	H_X	Average k_r/ 10^{-5} s^{-1}
X = X′ = H	1.52	1.51	1.99	1.7
X = X′ = m-Me	1.84	1.85	1.98	1.9
X = H, X′ = p-Me	3.11	3.20	3.33	3.2
X = H, X′ = p-MeO	4.49	4.52	4.50	4.5
X = H, X′ = p-Pr^{i}O	2.80	2.81	2.88	2.8
X = H, X′ = p-Et$_2$N	6.82	7.11	7.18	7.0

The magnitude of k_r increases with electron donation by X and a Hammett plot against σ gives $\rho = -0.9 \pm 0.5$. The correlation coefficient (0.90) is poor and thus the data should be regarded as a trend rather than a correlation. Nevertheless the implication is that electron donation accelerates betaine decomposition as well as betaine formation. The apparent paradox is resolved by noting that the *rate* of the back reaction is given by $k_{-1}[B] = k_{-1}[Y]/K_2$. Thus the reverse reaction must be dominated by the ylide/betaine interconversion since the positive ρ value for K_2 (0.4 ± 0.2) would then give a negative ρ value for the reverse reaction.

In conclusion the data may be used to create a reactivity profile embracing the rate of reaction (controlled by k_1, temperature and the medium) and the selectivity to DCB (controlled by K_2, the ratio k_8/k_5, temperature and the medium). From this it may be seen that the catalyst which gives the most convenient rate at 60 °C with a selectivity to DCB of *ca.* 92% is isopropyl di-p-tolylphosphinite. Moreover, under the reported experimental conditions, this catalyst gives a turnover in excess of 5000.

Acknowledgements

We are grateful to the EPSRC and to ICI Chemicals and Polymers, Wilton, Cleveland for CASE Awards to N. L. and B. R. T. and a summer studentship to A. C. H. We also thank Jane Hawkes and John Cobb for NMR spectra and the University of London Intercollegiate Research Service for NMR (KCL) and mass spectrometry (KCL and School of Pharmacy) data.

Appendix

Derivation of kinetic expressions

First consider the variation of [AN] *vs.* time. From Scheme 1, we obtain eqn. (*a*). Hence we require expressions for [B^1] and

$$-d[AN]/dt = k_1[P][AN] - k_{-1}[B^1] + k_5[B^1][AN] + k_8[Y][AN] \quad (a)$$

[Y]. In order to simplify the problem the equilibrium to P(v) was ignored since it is a non-productive process. Thus eqns. (*b*)

$$d[B^1]/dt = k_1[P][AN] - k_{-1}[B^1] - k_2[ROH][B^1] + k_{-2}[ROH][Y] - k_5[B^1][AN] \quad (b)$$

and (*c*) can be derived, while at the *steady state* eqn. (*d*) applies.

$$d[Y]/dt = k_2[ROH][B^1] - k_{-2}[ROH][Y] - k_8[Y][AN] \quad (c)$$

$$d[B^1]/dt = d[Y]/dt = 0 \quad (d)$$

This is justified by a ^{31}P NMR analysis of a dimerisation reaction where *no build up of phosphonium intermediates* is observed. Hence from eqns. (*b*) and (*c*) eqns. (e) and (*f*) can be

$$[Y] = K_2{}^*[B^1], \text{ where } K_2{}^* = k_2[ROH]/(k_{-2}[ROH] + k_8[AN]) \quad (e)$$

$$[B^1] = k_1[P][AN]/(k_{-1} + k_5[AN] + K_2{}^*k_8[AN]) \quad (f)$$

derived. Substitution for [B^1] and [Y] in eqn. (*a*) gives eqn. (*g*). From deuteriation studies we see that: $k_{-1} \ll k_5[\mathrm{AN}]$,

$$-\mathrm{d}[\mathrm{AN}]/\mathrm{d}t = 2k_1[\mathrm{P}][\mathrm{AN}](k_5[\mathrm{AN}] + k_8K_2^*[\mathrm{AN}])/(k_{-1} + k_5[\mathrm{AN}] + k_8K_2^*[\mathrm{AN}]) \qquad (g)$$

$k_8K_2^*[\mathrm{AN}]$. Hence $-\mathrm{d}[\mathrm{AN}]/\mathrm{d}t = 2k_1[\mathrm{P}][\mathrm{AN}]$. Thus plots of ln[AN] *vs.* time should reveal straight lines of slopes = $k_{\mathrm{obs}} = 2k_1[\mathrm{P}]$.

Now we consider the formation of dimers, DCB and MGN *vs.* time. For small k_{-1} and assuming that subsequent reactions through B^2 and B^3 are fast, then eqn. (*h*) applies for MGN, and eqn. (*i*) for DCB.

$$\begin{aligned}\mathrm{d}[\mathrm{MGN}]/\mathrm{d}t &= k_5[\mathrm{AN}][\mathrm{B}^1]\\ &= (k_5[\mathrm{AN}] \times k_1[\mathrm{P}][\mathrm{AN}])/(k_5[\mathrm{AN}] + K_2^*k_8[\mathrm{AN}])\\ &= k_1[\mathrm{P}][\mathrm{AN}]/(1 + K_2^*k_8/k_5) \qquad (h)\end{aligned}$$

$$\begin{aligned}\mathrm{d}[\mathrm{DCB}]/\mathrm{d}t &= k_8[\mathrm{AN}][\mathrm{Y}]\\ &= k_8K_2^*[\mathrm{AN}][\mathrm{B}^1]\\ &= (k_8K_2^*[\mathrm{AN}] \times k_1[\mathrm{P}][\mathrm{AN}])/(k_5[\mathrm{AN}] + K_2^*k_8[\mathrm{AN}])\\ &= K_2^*k_8k_1[\mathrm{P}][\mathrm{AN}]/k_5(1 + K_2^*k_8/k_5) \qquad (i)\end{aligned}$$

Now, $[\mathrm{DIMER}]_t = [\mathrm{DCB}]_t + [\mathrm{MGN}]_t$ and $2[\mathrm{DIMER}]_t = [\mathrm{AN}]_0 - [\mathrm{AN}]_t$. Since the ratio K_2k_8/k_5 is taken to reflect the observed ratio $[\mathrm{DCB}]_t/[\mathrm{MGN}]_t$ we obtain eqn. (*j*), and thus eqn. (*k*), which gives eqn. (*l*).

$$2[\mathrm{MGN}](1 + K_2k_8/k_5) = [\mathrm{AN}]_0 - [\mathrm{AN}]_t \qquad (j)$$

$$\mathrm{d}[\mathrm{MGN}]\mathrm{d}t = k_1[\mathrm{P}]\{[\mathrm{AN}]_0 - 2[\mathrm{MGN}](1 + K_2k_8/k_5)\}/(1 + K_2^*k_8/k_5) \qquad (k)$$

$$\mathrm{d}[\mathrm{MGN}]/[\mathrm{AN}]_0 - 2[\mathrm{MGN}](1 + K_2k_8/k_5) = k_1[\mathrm{P}]\mathrm{d}t/(1 + K_2^*k_8/k_5) \qquad (l)$$

Now, if k_{-2} [ROH] $\gg k_8$[AN] which is reasonable for a proton transfer process and confirmed by the rapid deuteriation in the olefinic sites of the isolated linear dimer, then from eqn. (*e*): $K_2^* \rightarrow K_2$. Using standard integrals [eqn. (*m*)] we derive the

$$\frac{\mathrm{d}x}{(b - ax)} = -\ln(b - ax)/a \qquad (m)$$

integrated rate equation, eqn. (*n*). From this, and assuming

$$\ln\{[\mathrm{AN}]_0 - 2[\mathrm{MGN}](1 + K_2k_8/k_5)\} = -2k_1[\mathrm{P}]t(1 + K_2k_8/k_5)/(1 + K_2k_8/k_5) = -2k_1[\mathrm{P}]t \qquad (n)$$

eqn. (*o*) applies, then eqn. (*p*) can be derived. By a similar

$$f[\mathrm{MGN}] = [\mathrm{AN}]_0 - 2[\mathrm{MGN}](1 + K_2k_8/k_5) \qquad (o)$$

$$\ln f[\mathrm{MGN}] = -2k_1[\mathrm{P}]t \qquad (p)$$

argument we obtain eqn. (*q*), where $f[\mathrm{DCB}] = [\mathrm{AN}]_0 -$

$$\ln f[\mathrm{DCB}] = -2k_1[\mathrm{P}]t \qquad (q)$$

$2[\mathrm{DCB}](1 + k_5/K_2k_8)$. Hence the plots of f[DCB] and f[MGN] *vs.* time should reveal straight lines of slopes = $k_{\mathrm{obs}} = 2k_1[\mathrm{P}]$.

Therefore we have *three* routes to the value of k_1 through monitoring the consumption of AN and the formation of both the linear and branched dimers. Also, from the ratio $[\mathrm{DCB}]_t/[\mathrm{MGN}]_t$ we can assess a value of the ratio K_2k_8/k_5. However, the above kinetic analysis essentially *ignores* any pathway giving rise to the small quantities of oligomer (normally trimer and crystalline hexamers) that are observed during a dimerisation reaction. Thus the 'raw' $[\mathrm{AN}]_t$, $[\mathrm{MGN}]_t$ and $[\mathrm{DBC}]_t$ data were refined by the incorporation of small corrections which were dependent on the knowledge of the *origin* and *quantities* of both trimer and hexamer.

References

1 (*a*) J. D. McClure, *J. Org. Chem.*, 1970, **35**, 3045; (*b*) R. Oda, T. Kawabata and S. Tanimoto, *Tetrahedron Lett.*, 1964, 1653; (*c*) P. D. Beer, R. C. Edwards, C. D. Hall, J. R. Jennings and R. J. Cozens, *Phosphorus Sulfur*, 1983, **17**, 283; (*d*) C. D. Hall, N. Lowther, B. R. Tweedy, R. Kayhanian, M. Piffl and G. Shaw, *Phosphorus, Sulfur Silicon*, 1996, **109–110**, 521.

2 J. R. Jennings and R. J. Cozens, *Appl. Catalysis A*, 1995, **124**, 297.

3 J. R. Jennings, R. J. Cozens and K. Wade, *Appl. Catalysis A*, 1995, **130**, 175.

4 J. R. Jennings and R. J. Cozens, *Appl. Catalysis A*, 1996, **135**, 163.

5 A. I. Vogel, *A Textbook of Practical Organic Chemistry*, 1956, Longmans, London.

6 C. D. Hall, B. R. Tweedy and N. Lowther, *Phosphorus, Sulfur Silicon*, 1997, **123**, 341.

7 J. R. Lloyd, N. Lowther and C. D. Hall, *J. Chem. Soc., Perkin Trans. 2*, 1985, 245.

8 J. R. Lloyd, N. Lowther, G. Szabo and C. D. Hall, *J. Chem. Soc., Perkin Trans. 2*, 1985, 1813.

9 C. D. Hall, P. D. Beer, R. L. Powell, M. P. Naan, *Phosphorus, Sulfur Silicon*, 1995, **105**, 145.

10 G. P. Schiemenz, *Chem. Ber.*, 1966, **98**, 514.

11 F. G. Mann and I. G. Millar, *J. Chem. Soc.*, 1952, 4453.

12 W. H. Dietsche, *Tetrahedron Lett.*, 1966, 6347.

13 M. G. Futica and H. J. Harwood, *J. Macromol. Sci., Chem.*, 1978, **A12**, 1099.

Paper 7/07559F
Received 20*th October* 1997
Accepted 3rd *June* 1998